Pyrite ooids in Devonian black shales record intermittent sea-level drop and shallow-water conditions

Jürgen Schieber Department of Geological Sciences, Indiana University, Bloomington, Indiana 47405, USA
Lee Riciputi Chemical and Analytical Services Division, Oak Ridge National Laboratory, P.O. Box 2008, Oak Ridge, Tennessee 37831-6365, USA

ABSTRACT

Upper Devonian black shales of the eastern United States contain in places unusual beds of pyrite ooids. Textural and geochemical studies show that these originated as chamositic iron ooids that were replaced by pyrite during early diagenesis. Pyrite mimics the laminated texture of the precursor grain, yet inclusions of silicate minerals and instances of partial replacement reveal the secondary nature of the pyrite. Pyrite ooids occur above erosion surfaces that are considered sequence boundaries because of large lateral extent. Chamositic precursor ooids indicate an oxygenated water column and wave interaction with seafloor sediments at the time of their formation. This scenario agrees with earlier work that stipulates that erosion surfaces in Devonian black shales reflect lowering of sea level that allowed wave reworking and erosion of earlier-deposited black shales. Pyrite ooid beds thus furnish direct evidence of significant sea-level drops during the accumulation of Upper Devonian black shales in eastern North America.

Keywords: black shale, sea level, sequence boundary, pyrite ooids, chamosite, ironstone.

INTRODUCTION

Upper Devonian black shales of the eastern United States have long been thought of as having been deposited in the deepest parts of stagnant basins (e.g., Kepferle, 1993; Ettensohn et al., 1988; Potter et al., 1982). Closer examination, however, reveals a more complex picture. Although there are undoubtedly deep-basin deposits in some areas, there is good evidence that in other areas these black shales were deposited in shallow water, within reach of storm waves and with abundant benthic life (Schieber, 1998a; Lobza and Schieber, 1999). Outcrops in Tennessee and Kentucky show extensive erosion surfaces within the Chattanooga and New Albany Shales that allow sequence stratigraphic subdivision of this succession. Individual sequences onlap the Cincinnati Arch, and are deeply eroded or even removed over the crest of the arch (Schieber, 1998b; Johri and Schieber, 1999). These geometric relationships implicate sea-level drop as a major factor in the production of sequence-bounding erosion surfaces.

Pyrite ooid beds (typically <10 cm in thickness) occur on top of erosion surfaces that cut down into the underlying black shales (Schieber, 1998a). Contacts between pyrite ooid beds and underlying black shales are sharp, and multiple scour surfaces within pyrite ooid beds indicate a prolonged history of high-energy reworking and winnowing. The strong grain-size contrast between black shale and pyrite ooid beds (coarse sand) also indicates that pyrite ooid beds formed in considerably shallower water than did black shales.

The smooth oval-rounded outline of ooids (Fig. 1), the fine detail of concentric laminae of pyrite, and the apparent accretion of pyrite cortices on initial cores (pyrite, phosphatic debris, quartz) give an initial impression of a primary (at the sediment surface) rather than diagenetic (postdepositional) origin. We show that these pyrite ooids originated when chamositic iron ooids, produced during lowstand reworking, were pyritized after being covered with organic-rich muds during sea-level rise. The pyrite ooids therefore provide new independent evidence for sea-level drop as a cause for erosion surfaces within Upper Devonian black shales of the eastern United States.

Other examples of pyrite ooid beds are known from the Devonian of the Williston Basin, the Ordovician of Newfoundland, the Cambrian of Iowa, and from a variety of oolitic ironstone deposits. Pyritic ooids are readily destroyed during weathering and petrographic thin sections are required for their identification. It is therefore likely that pyrite ooid–bearing intervals and the sea-level variations that they indicate will be recognized in future studies of other black shale successions.

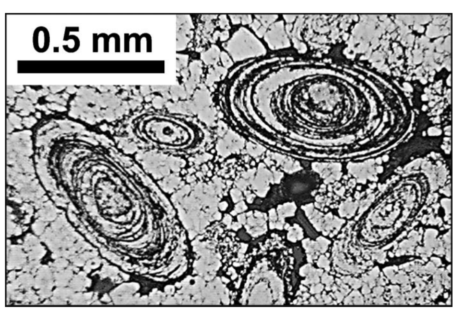

Figure 1. Pyrite ooids in pyritic lag deposit from Chattanooga Shale in Tennessee (location 1, Fig. 2). Note coarse crystalline pyrite cement (light color) between ooids.

METHODS

Samples were collected from outcrops of the Gassaway Member of the Chattanooga Shale (Famennian, central Tennessee) and from a drill core of the New Albany Shale in Jackson County, southern Indiana (Fig. 2). The Gassaway samples were studied in considerable detail by reflected-light microscopy, scanning electron microscope (SEM including energy-dispersive X-ray microanalysis), electron microprobe (JEOL JXA-733 Superprobe), ion microprobe (Cameca 4f, S isotopes), and laser-ablation mass spectroscopy (S isotopes). Pyrite ooids in the New Albany Shale were discovered after the analytical work on the Tennessee samples had already been completed and were examined by reflected-light microscopy to establish their textural unity with samples from Tennessee.

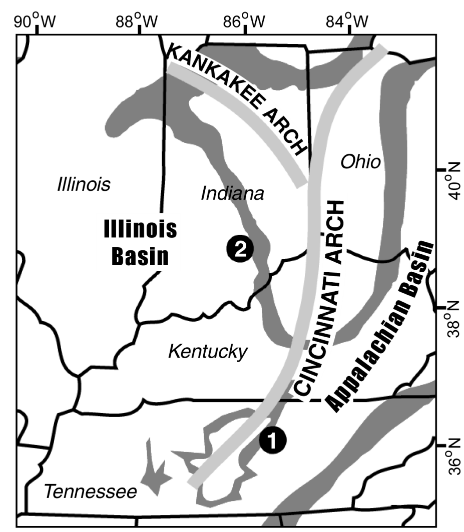

Figure 2. Location map, showing study region, outcrop belt of Devonian black shale (dark gray), major structural elements (Cincinnati and Kankakee Arches, light gray), Appalachian and Illinois Basins, and sample locations (black circles). Location 1 shows occurrence of pyrite ooids (outcrop samples) along eastern highland rim in Tennessee, and location 2 shows occurrence from Jackson County, Indiana (core material).

OBSERVATIONS

Petrography

The great majority of ooids from Tennessee show well-developed, finely crystalline, pyritic cortices (Fig. 1) that enclose a core of variable composition (reworked and rounded diagenetic pyrite grains, phosphatic fossil debris, pyrite ooids, pyrite ooid fragments). These ooids are overgrown and cemented with coarse crystalline pyrite and may show replacement by coarse crystalline pyrite along the margins. Replacement of fine crystalline pyrite cortices by coarse crystalline pyrite along the margins, pyrite ooid cores, broken pyrite ooids that are overgrown by more pyrite laminae, and internal truncation of laminae (cortex unconformities), as well as the conformable and fine crystalline nature of the cortices, are all consistent with a primary origin of the pyrite ooids. In some places, however, pyrite ooids show deformation, fracture, and collapse of pyritic cortices (Fig. 3A), suggestive of a softer precursor material. In addition, SEM examination of cortex surfaces showed in places irregular thin patches of iron-bearing clay minerals (Fig. 3C), with the clay platelets oriented parallel to the cortex surface. Internal stratification within pyrite ooid beds shows disruption due to bioturbation.

In the Frasnian occurrence from Indiana, ooids with pyritic cortices are also common. In addition, however, there are abundant grains that consist entirely of chamosite, as well as intermediaries that leave no doubt about the secondary nature of the pyritic cortices (Fig. 3B).

Microprobe Data

Because replacement of one mineral phase by another is rarely perfect, we assumed that secondary (replaced) pyrite ooids should evidence this process through silicate mineral inclusions within the pyrite cortices. Although such inclusions were not observed in polished thin sections from the Tennessee occurrence, electron-microprobe analysis of a number of pyrite ooids showed a persistent background of several percent of SiO_2 and Al_2O_3 (Fig. 4A).

Sulfur Isotope and Ion-Microprobe Data

Pyrite ooids as well as the coarser crystalline pyrite matrix between them (Fig. 1) were analyzed for sulfur isotope ratios via laser-ablation mass spectrometry and ion microprobe. Sulfur isotope data (in delta notation, relative to Cañon Diablo troilite) for both analytical approaches are in good agreement. Ion-microprobe measurements of $\delta^{34}S$ values in sulfur average −22.2‰ for cortical pyrite (10 measurements, range −21.9‰ to −28.9‰) and −13.3‰ for matrix pyrite (6 measurements, range −9.3‰ to −19.1‰). Laser-ablation $\delta^{34}S$ measurements average −22.7‰ for cortical pyrite (4 measurements, range −19.9‰ to −26.1‰) and −13.5‰ $\delta^{34}S$ for matrix pyrite (4 measurements, range −9.1‰ to −16.4‰). Both methods show that matrix pyrite is ~9‰ more enriched in ^{34}S than the cortical pyrite. Where we were able to make multiple measurements of cortical pyrite, the sulfur isotope values fall within a narrow range (Fig. 4B).

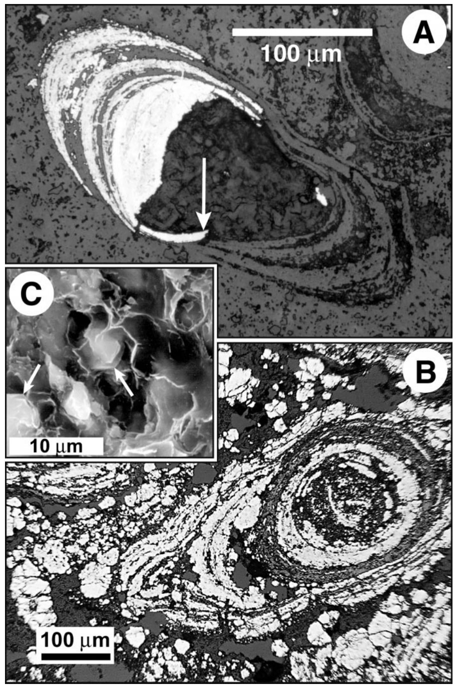

Figure 3. A: Partially replaced chamosite ooid from location 2 (pyrite—light colored, chamosite cortices—medium gray). Cracked pyrite lamina (white arrow) and contrast in deformation between pyritic (left) and chamositic (right) half of ooid indicate early pyritization, prior to compaction. B: Pyrite ooid with deformed and crushed cortices from location 1. Crushed pyrite laminae (light color) suggest that some softer material was present between pyrite laminae and was possibly dissolved or squeezed out during compaction. These observations indicate that pyritization occurred early in diagenetic history and prior to compaction. "Soft" material may have been berthierine, chamosite precursor mineral. C: Scanning electron microscope image from patch of cortex-parallel iron-bearing clay minerals in pyrite ooid from location 1, presumably remnant of original grain.

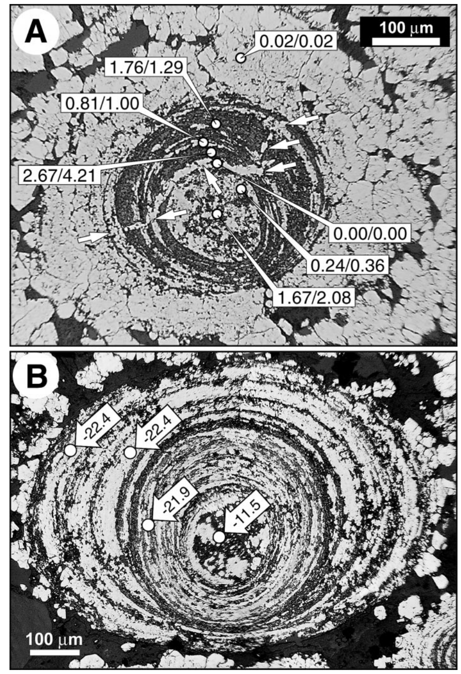

Figure 4. A: Electron-microprobe analysis of pyrite ooid from location 1. Probe spots marked with white circles; numbers in boxes are values for SiO_2 (left) and Al_2O_3 (right). Late fracture that cuts across ooid (marked by short white arrows) is free of silicate inclusions, similar to later diagenetic, blocky, interooid pyrite cement. B: Ion-microprobe sulfur isotope data for pyrite ooid from location 1. Probe spots are marked with white circles; number in arrow is measured $\delta^{34}S$ value. Note narrow range of $\delta^{34}S$ values for cortical pyrite. $\delta^{34}S$ value of core region differs significantly from that observed in cortices and is essentially same as measured in late-diagenetic interooid pyrite cement. This indicates that ooid core was pyritized later in diagenesis, some time after pyritization of cortices.

Origin of Pyrite Ooids

While initial examination of pyrite ooids from Tennessee (Fig. 1) suggested primary formation on the Devonian seafloor, replacement of a concentrically laminated precursor grain was pursued as an alternative hypothesis. Potential precursor grains are either carbonate ooids or iron ooids from oolitic ironstones, and a carbonate precursor was ruled out due to a lack of carbonate inclusions and associated carbonate rocks.

Pyrite ooids from Tennessee show a ''flattened,'' ellipsoidal shape (Fig. 1) due to equatorial thickening of cortical sheets. This feature is characteristic of chamositic iron ooids worldwide (Carozzi, 1972; Maynard, 1983; Siehl and Thein, 1989), as well as for Devonian chamositic ooids in Iowa, New York, and elsewhere on the North American craton (Van Houten, 1990). Deformational features, such as crushed and squeezed cortices (Fig. 3A), are also common in chamosite ooids (Kimberley, 1983). Because of a paucity of petrographic evidence for replacement we also looked for more subtle hints, such as submicroscopic inclusions of Al silicates. We assumed that the latter should cause elevated levels of Si and Al in cortical pyrite, and confirmed this hypothesis with electron microprobe data (Fig. 4A). Whereas pyrite cement and late diagenetic fracture fill pyrite contain little or no Si and Al, SiO_2 and Al_2O_3 contents in cortical pyrite reach 2.67% and 4.21%, respectively. Measurements on a large number of ooids indicate that values in this range are typical, suggesting replacement of a precursor Al silicate. In contrast, ooids with supposedly primary pyrite cortexes lack detectable levels of Si and Al (Schieber, 1999) and are devoid of mineral inclusions (Pufahl and Grimm, 2003). Furthermore, pyrite ooids from location 1 (Fig. 2) contain cortex-parallel patches of iron-bearing clay minerals (Fig. 3C) that are probably remnants of original grains. Being an iron-bearing clay mineral, chamosite is a good candidate for this precursor material.

Given a 0.5‰ reproducibility of ion microprobe $\delta^{34}S$ measurements (Riciputi et al., 1998), $\delta^{34}S$ values for the laminated parts of pyrite ooids (Fig. 4B) can be considered uniform. This implies an essentially constant composition of mineralizing fluids and indicates replacement. Had pyrite cortices accreted successively over time, e.g., as redox-aggraded grains (Pufahl and Grimm, 2003) due to vertical oscillations of the redox interface through an organic-rich surface sediment, it would be reasonable to expect a certain amount of $\delta^{34}S$ variability between cortices.

Crushed pyrite cortices (Figs. 3A, 3B) indicate pyritization early in diagenetic history, prior to compaction. The $\delta^{34}S$ values of cortical pyrite support this notion. They are quite negative (−22‰), strongly fractionated relative to Late Devonian marine sulfates ($\delta^{34}S$ = +25‰ to +30‰; Claypool et al., 1980), and suggest early diagenetic microbial sulfide reduction and open-system conditions. In contrast, the less-negative $\delta^{34}S$ values (−13‰) of the pyrite cement between ooids are consistent with later emplacement after some burial (Strauss and Schieber, 1989).

Pyrite ooids from location 2 (Fig. 2) have the same ''flattened'' ellipsoidal shape as those from location 1 (Fig. 1). Combined with the textural likeness between the two occurrences, the discovery of only partially pyritized chamosite ooids (Fig. 3B) in location 2 provides additional support for interpreting the pyrite ooids from location 1 as replaced chamosite ooids.

IMPLICATIONS

Finding that pyrite ooids in Devonian black shales of Indiana and Tennessee formed via diagenetic replacement of chamosite ooids implies that pyrite ooid beds have to be viewed as diagenetically altered oolitic ironstones. Current understanding of oolitic ironstones (Maynard, 1983; Young, 1989; Hallam, 1975) suggests that these beds originally formed in shallow, wave-agitated water. In a survey of oolitic ironstones, Van Houten and Bhattacharyya (1982) concluded that they form at the top of shoaling-upward sequences (relative sea-level drop) and are in turn covered by transgressive marine mudstones. The chamosite (Fig. 3B) in these ooids forms from precursor berthierine during burial diagenesis (Young, 1989). Because berthierine formation requires mildly reducing conditions, the ooids imply multiple episodes of intrasediment berthierine growth (i.e., within a blanket of reworked surface sediment), interrupted by intermittent exhumation and reworking (Young, 1989).

The black shales with pyrite ooid beds contain evidence of storm-wave reworking (Schieber, 1994), suggesting a water depth on the order of tens of meters (Schieber, 1998a). This is comparatively shallow, but nonetheless was deep enough to allow accumulation of mud. Pyrite ooid beds occur on major erosion surfaces, contain other coarse grains (e.g., quartz, conodonts, pyrite concretions), have been winnowed of clays, and clearly formed in shallower water than did the black shales. Thus, although they are quite a bit thinner (10 cm) than typical oolitic ironstones (on the order of meters), the precursor ooid beds nonetheless formed in an environment (shallow, wave agitated) that compares well with what is envisioned for oolitic ironstones.

Pyrite ooid beds that are intercalated with Upper Devonian black shales imply the following sequence of events: (1) black shale deposition; (2) lowering of sea level and partial erosion of previously deposited black shale; (3) formation of berthierine/chamosite ooids on erosion surface; (4) renewed sea-level rise and onset of black shale deposition; (5) pyritization of berthierine/chamosite ooids as they are blanketed by carbonaceous muds; and (6) burial beneath more black shale. At step 5, a thin blanket of carbonaceous mud still allows seawater sulfate to diffuse into the now-reducing sediment, leading to strongly negative $\delta^{34}S$ values of pyritized ooid cortices. Once the black shale cover gets too thick (step 6), downward diffusion of seawater sulfate is strongly impeded (closed-system conditions), resulting in the more positive $\delta^{34}S$ values of pyrite cement (Strauss and Schieber, 1989).

In typical oolitic ironstones the iron is derived from the adjacent landmass (Maynard, 1983). However, because our pyrite ooid beds occur along the flanks of the Cincinnati Arch (Fig. 2), far removed from any shoreline, the Devonian black shales were the most likely source of iron. Erosion and reworking of these black shales, which contain on average an equivalent of 5% Fe_2O_3, would have exposed their pyrite content to oxidation and provided iron in the form of iron hydroxides, the likely main source of iron in marine oolitic ironstones (Young, 1989). Wave reworking associated with lowstand conditions would have provided a suitable environment for ooid formation.

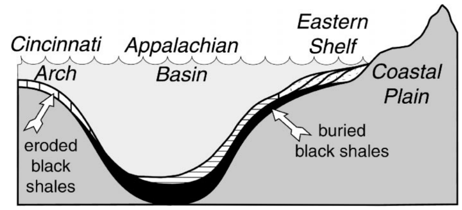

Figure 5. Effect of sea-level drop on black shales that onlap eastern shelf of Appalachian Basin and on black shales on Cincinnati Arch. Along eastern basin margin, coastal plain and inner shelf erosion and basinward progradation of clinoforms bury previously deposited black shales and protect them from erosion. For Cincinnati Arch, sediment input from east is trapped in Appalachian trough, and main effect of sea-level drop is that it brings previously deposited black shales within reach of wave reworking. Thus, shale erosion dominates Cincinnati Arch region.

In a study of black shale–associated erosion surfaces from the Middle Devonian of New York State, Baird and Brett (1986, 1991) concluded that widespread erosion occurred in times of sea-level rise and was due to shoaling internal waves that traveled along the pycnocline. Their conclusion seems to be at odds with our model of sea-level drop as a cause for erosion surfaces in Upper Devonian black shales of the Cincinnati Arch region (Schieber, 1998b). The ostensible contradiction between the two models, however, can in essence be reduced to a difference in location. Changes of basin configuration from the Middle to Upper Devonian may be an additional factor. The major difference between the two models seems to be that erosion surfaces on the Cincinnati Arch formed far removed from the input of clastics along the eastern basin margin, whereas those in New York State formed much closer to its eastern shoreline. Sea-level drop has a very different effect for the two areas, causing black shale erosion on the Cincinnati Arch and black shale burial along the eastern basin margin (Fig. 5). Because of proximity to sediment input, the erosion surfaces from New York State described by Baird and Brett (1986) can probably only form during times of sea-level rise, when sediment trapping by a transgressive shoreline promotes offshore sediment starvation and formation of submarine erosion surfaces by either internal or storm waves. At those times of rising sea level, sedimentation on the Cincinnati Arch was dominated by deposition of highly carbonaceous black shales (transgressive shales of Ettensohn et al., 1988) and possibly by hiatal deposits enriched in authigenic silica and pyrite (Schieber, 1998a).

Pyrite ooids associated with carbonaceous shales also occur in the Devonian of the Williston Basin (P. Binda, 1998, personal commun.), and the Ordovician of Newfoundland (Hayes, 1915; Ranger et al., 1984). In the latter occurrence pyrite ooid beds are interstratified with laminated carbonaceous shales that were deposited in a deeper water setting. Scoured bases, cross-bedding, hummocky cross-stratification, and *Cruziana*-style bioturbation clearly show that the pyrite ooid beds were deposited in shallower water than were the enclosing shales. Partially pyritized chamosite ooids indicate that Fe ooids were washed in from ironstone shoals during lowering of sea level (Ranger, 1979) and then buried under carbonaceous muds as sea level rose. Pyrite ooids in the Cambrian Mt. Simon Sandstone of Iowa occur in a succession of interstratified sandstones and mudstones. Prominent pyrite ooid beds rest on sharp erosional bases, potential sequence boundaries. These observations suggest that pyrite ooids may find general application as an indicator of significant sea-level variation in successions that otherwise would be considered to record stable (uniform) conditions.

CONCLUSION

Pyrite ooid beds in Upper Devonian black shales represent diagenetically altered chamositic ironstones. These ooid beds indicate significant intermittent drops of sea level during deposition of Upper Devonian black shales in the eastern United States. They also provide independent confirmation of an earlier-proposed model (Schieber, 1998b), in which erosion surfaces in Upper Devonian black shales of the Cincinnati Arch region are explained as a result of erosion due to lowered sea level. The latter model is not in conflict with one by Baird and Brett (1991) that explains erosion recorded in Middle Devonian black shales of the eastern Appalachian Basin as a result of transgression and sediment starvation. The seeming contradiction between the two models derives from the fact that we have contrasting expressions of sea-level rise and sea-level fall between the sediment-starved Cincinnati Arch region and the well-supplied eastern margin of the Appalachian Basin. Because pyrite ooids in black shales easily escape detection due to weathering, they are probably more widespread than currently known and may yet find wider application as an indicator of sea-level drop.

ACKNOWLEDGMENTS

Research on pyrite ooids in the Chattanooga Shale was supported by the National Science Foundation (grant EAR-9706178). Acknowledgment is also made to the donors of the Petroleum Research Fund, administered by the American Chemical Society (ACS-PRF grant 25134-AC2), for supporting the fieldwork component of this research. Helpful suggestions by reviewers G. Baird and P. Pufahl improved the clarity of presentation.

REFERENCES CITED

Baird, G.C., and Brett, C.E., 1986, Erosion on an anaerobic seafloor: Significance of reworked pyrite deposits from the Devonian of New York: Palaeogeography, Palaeoclimatology, Palaeoecology, v. 57, p. 157–193.

Baird, G.C., and Brett, C.E., 1991, Submarine erosion on the anoxic sea floor: Stratinomic, palaeoenvironmental, and temporal significance of reworked pyrite-bone deposits, *in* Tyson, R.V., and Pearson, T.H., eds., Modern and ancient continental shelf anoxia: Geological Society [London] Special Publication 58, p. 233–257.

Carozzi, A.V., 1972, Microscopic sedimentary petrography: Melbourne, Florida, Krieger Publishing Company, 485 p.

Claypool, G.E., Holser, W.T., Kaplan, I., Sakai, H., and Zak, I., 1980, The age curves of sulfur and oxygen isotopes in marine sulfate and their mutual interpretation: Chemical Geology, v. 28, p. 199–260.

Ettensohn, F.R., Miller, M.L., Dillman, S.B., Elam, T.D., Geller, K.L., Swager, D.R., Markowitz, G., Woock, R.D., and Barron, L.S., 1988, Characterization and implications of the Devonian–Mississippian black shale sequence, eastern and central Kentucky, U.S.A.: Pycnoclines, transgression, regression, and tectonism, *in* McMillan, N.J., et al., eds., Devonian of the world, Volume 2: Canadian Society of Petroleum Geologists Memoir 14, p. 323–345.

Hallam, A., 1975, Jurassic environments: Cambridge, Cambridge University Press, 269 p.

Hayes, A.O., 1915, Wabana iron ore of Newfoundland: Canada Geological Survey Memoir 78, 162 p.

Johri, P., and Schieber, J., 1999, A regional study of sequences in the New Albany Shale of the southeastern Illinois Basin (Indiana) with gamma ray logs and well cores, *in* Merriam, D.F., ed., America Association of Petroleum Geologists regional meeting in Wichita, Kansas, Transactions of the 1999 AAPG Midcontinent Section Meeting: Kansas Geological Survey Open-File Report 99-28, p. 211.

Kepferle, R.C., 1993, A depositional model and basin analysis for the gas-bearing black shale (Devonian and Mississippian) in the Appalachian Basin: U.S. Geological Survey Bulletin 1909, p. F1–F23.

Kimberley, M.M., 1983, Ferriferous ooids, *in* Peryt, T., ed., Coated grains: Berlin, Springer-Verlag, p. 100–108.

Lobza, V., and Schieber, J., 1999, Biogenic sedimentary structures produced by worms in soupy, soft muds: Observations from the Chattanooga Shale (Upper Devonian) and experiments: Journal of Sedimentary Research, v. 69, p. 1041–1049.

Maynard, J.B., 1983, Geochemistry of sedimentary ore deposits: New York, Springer Verlag, 305 p.

Potter, P.E., Maynard, J.B., and Pryor, W.A., 1982, Appalachian gas bearing Devonian shales: Statements and discussions: Oil and Gas Journal, v. 80, p. 290–318.

Pufahl, P.K., and Grimm, K.A., 2003, Coated phosphate grains: Proxy for physical, chemical, and ecological changes in seawater: Geology, v. 31, p. 801–804.

Ranger, M.J., 1979, The sedimentology of a lower Paleozoic peritidal sequence associated iron formations, Bell Island, Conception Bay, Newfoundland [M.S. thesis]: St. Johns, Newfoundland, Memorial University of Newfoundland, 125 p.

Ranger, M.J., Pickerill, R.K., and Fillion, D., 1984, Lithostratigraphy of the Cambrian?—Lower Ordovician Bell Island and Wabana Groups of Bell, Little Bell, and Kellys islands, Conception Bay, eastern Newfoundland: Canadian Journal of Earth Sciences, v. 21, p. 1245–1261.

Riciputi, L.R., Paterson, B.A., and Ripperdan, R.L., 1998, Measurement of light stable isotope ratios by SIMS: Matrix effects for oxygen, carbon and sulfur isotopes in minerals: International Journal of Mass Spectrometry, v. 178, p. 81–112.

Schieber, J., 1994, Evidence for episodic high energy events and shallow water deposition in the Chattanooga Shale, Devonian, central Tennessee, U.S.A.: Sedimentary Geology, v. 93, p. 193–208.

Schieber, J., 1998a, Sedimentary features indicating erosion, condensation, and hiatuses in the Chattanooga Shale of Central Tennessee: Relevance for sedimentary and stratigraphic evolution, *in* Schieber, J., et al., eds., Shales and mudstones, Volume 1: Stuttgart, Schweizerbart'sche Verlagsbuchhandlung, p. 187–215.

Schieber, J., 1998b, Developing a sequence stratigraphic framework for the Late Devonian Chattanooga Shale of the southeastern US: Relevance for the Bakken Shale, *in* Christopher, J.E., et al., eds., Eighth International Williston Basin Symposium: Saskatchewan Geological Society Special Publication 13, p. 58–68.

Schieber, J., 1999, Pyrite ooids and oncoids from the Winnipeg Formation (Ordovician of Saskatchewan): Textural and geochemical observation in support of a primary origin: Geological Society of America Abstracts with Programs, v. 31, no. 7, p. A282.

Siehl, A., and Thein, J., 1989, Minette-type ironstones, *in* Young, T.P., and Taylor, W.E.G., eds., Phanerozoic ironstones: Geological Society [London] Special Publication 46, p. 175–193.

Strauss, H., and Schieber, J., 1989, A sulfur isotope study of pyrite genesis: The Mid-Proterozoic Newland Formation, Belt Supergroup, Montana: Geochimica et Cosmochimica Acta, v. 54, p. 197–204.

Van Houten, F.B., 1990, Phanerozoic oolitic ironstones on the North American craton: Palaeogeography, Palaeoclimatology, Palaeoecology, v. 80, p. 245–254.

Van Houten, F.B., and Bhattacharyya, D.P., 1982, Phanerozoic oolitic ironstones—Geologic record and facies model: Annual Reviews of Earth and Planetary Sciences, v. 10, p. 441–457.

Young, T.P., 1989, Phanerozoic ironstones: An introduction and review, *in* Young, T.P., and Taylor, W.E.G., eds., Phanerozoic ironstones: Geological Society [London] Special Publication 46, p. ix–xxv.

Manuscript received 13 September 2003
Revised manuscript received 23 December 2003
Manuscript accepted 24 December 2003

Printed in USA